A mathematical model for a lithium-polymer cell based on a lumped parameter representation of the charge diffusion process

Augusto de Holanda B. M. Tavares *
Florian vor dem Esche ** **Saulo O. D. Luiz** *
Florian Holzapfel ** **Antonio M. N. Lima** *

* *Electrical Engineering Department, Federal University of Campina Grande, Brazil (e-mails: augusto.tavares@ee.ufcg.edu.br, {saulo, amnlima}@dee.ufcg.edu.br).*
** *Institute of Flight System Dynamics, Technische Universität München, Germany (e-mails: {florian.vordemesche, florian.holzapfel}@tum.de).*

Abstract: This paper proposes a model for Lithium-Polymer batteries with diffusion dynamics through a lumped parameter approach in conjunction with an electrical model. A comparison of the performance of several optimization approaches to identify the model parameters from experimental tests is also conducted. Constant and pulsed current discharge experiments were performed on a set of three battery cells using a programmable DC load. The resulting data sets were used to obtain several model parameters using different optimization approaches. The predicted outputs of a discrete battery model using the parameters estimated by each algorithm were compared against the experimental data. The resulting models had an overall good performance, proving that the chosen modelling approach is applicable to Lithium-Polymer batteries, and that the choice of algorithm to identify the system parameters must be made with care.

Keywords: Lithium-Polymer batteries, Nonlinear system identification, Optimization, Nonlinear modelling, Control oriented models

1. INTRODUCTION

Lithium-ion (Li-ion) and Lithium polymer (LiPo) batteries have become a common choice for energy storage solutions in applications such as electrical vehicles, portable electronic devices and renewable energy power plants, due to their high energy density, small size and prolonged lifetime. As such, obtaining accurate models for these devices is paramount for these applications, as the power source tends to be a critical component of any system (Valladolid et al. (2019)). The model for lithium polymer batteries was formulated by Doyle et al. (1993), where electrochemical differential equations where used to describe the behavior of the relevant physical variables.

Since then, other models have been proposed, aiming to provide less computationally intensive solutions (Schmidt et al. (2010)) or to model effects such as battery aging (Daigle and Kulkarni (2013)). In Rakhmatov and Vrudhula (2001) a model for the diffusion dynamics of a Li-ion battery was defined using a lumped parameter approach, proving itself able to predict battery discharge times at a low computational cost, and further work was done by Neves et al. (2016) to represent this model by means of the Laplace transform.

Considering that the battery behavior is nonlinear, either experiments must be performed such that they can be identified by means of an optimization algorithm (Cipin et al. (2019)), or the system parameters must be previously known in the case of electrochemical models. As the available battery models differ significantly, the estimation problem itself is of research interest (Peng et al. (2018)), since several questions must be answered to obtain a reliable model: which experiments need to be performed, how accurate is the resulting model and what is the relative performance between different optimization techniques.

Within this scope of research, this paper presents the following contributions:

- A model for a Lithium-Polymer battery using the Rakhmatov-Vrudhula diffusion dynamics along with an electrical model is proposed, and its performance is verified against experimental results.
- An experimental demonstration that the diffusion coefficient for the Rakhmatov-Vrudhula model needs to be re-estimated to properly model the recovery effect of the battery.

⋆ This study was financed in part by the Coordenação de Aperfeiçoamento de Pessoal de Nível Superior - Brasil (CAPES) and the UFCG Post-graduate Program of Electrical Engineering (PPgEE) - Finance Code 001.

- A comparison between the performance of different numerical approaches for the estimation of the parameters of the proposed model.

This paper is organized as follows: a brief literature review is provided in Section 2, the battery model is described in Section 3, the experimental results and model behavior are presented in Section 4, and a conclusion indicating future research avenues can be found in Section 5.

2. RELATED WORKS

The model proposed in Doyle et al. (1993) uses a distributed parameter approach to model the electrochemical and transport phenomena inside of a lithium-polymer battery (Mazumder and Zhang (2013)), admitting multiple chemical compositions for the battery construction. However, the model results in a set of coupled differential equations, which demand a computationally intensive numerical solution, while also needing the knowledge of several of the constructive parameters of the battery.

These factors lead to limitations in the applicability of the model, which were explored by previous authors. In works such as Mazumder and Zhang (2013), Schmidt et al. (2010) and Daigle and Kulkarni (2013) models which try to capture the intricate electrochemical phenomena while being feasible for real-time applications are proposed. In Lee et al. (2018), Afshari et al. (2018) and Wang et al. (2020) the authors are not necessarily interested in modelling the internal dynamics of the battery, instead aiming to provide accurate predictions of the battery state of charge and voltage, for use in state estimation in control applications in vehicles and other systems.

Other authors are concerned with different effects that might affect the battery performance. This is the case in Barcellona and Piegari (2021), Valladolid et al. (2019) and Muratori et al. (2010), which explore how the effects and modelling of the temperature of LiPo batteries during discharge. In Guo et al. (2019), Chen et al. (2019) and Junhuathon et al. (2020) the authors are concerned with the effects of aging as the battery cells are discharged and recharged over time.

The model proposed in this paper combines the diffusion model of Rakhmatov and Vrudhula (2001) with an electrical model. The coupling of an electrical model to a model that gives an estimation of the state of charge is a widely used strategy in battery modelling, as can be seen in Lee et al. (2018), Valladolid et al. (2019) and Wang et al. (2022).

The Rakhmatov-Vrudhula diffusion model has been used to model the diffusion dynamics of Li-ion batteries in works such as Wang et al. (2022), Neves et al. (2016) and Spohn et al. (2008), and provides an accurate solution to the state of charge estimation problem coupled with a very low computational cost. The resulting model is a solution for the differential equations that describe the diffusion that's dependent solely on the knowledge of the total battery capacity and the diffusion coefficient. Upon studying the mechanisms of LiPo batteries described in Doyle et al. (1993), and used in other models for these types of batteries, it was verified that the Rakhmatov-Vrudhula model employs a similar physical description of the diffusion phenomenon that acts as the transport mechanism for the lithium ions inside the battery. This led to the hypothesis that the Rakhmatov-Vrudhula model lumped parameter solution can also be used to model the diffusion in LiPo batteries.

3. MODEL OF A LITHIUM-POLYMER BATTERY

In this section, the battery model used in this work is presented, being constituted by the combination of a diffusion model (Rakhmatov and Vrudhula (2001) and Neves et al. (2016)) and an electrical model. A discrete-time version of this battery model used in the parameter identification process is also shown. The proposed model combination intends to provide an accurate reproduction of the effects of the internal battery dynamics over the battery voltage and state of charge, while also being computationally efficient and identifiable from a series of relatively simple experiments.

3.1 Diffusion model

The diffusion model is described in (1) and (2), where α is the total battery capacity in C, β is the diffusion coefficient in $s^{-\frac{1}{2}}$ and is a value between 0 and 1, i_b is the battery current in A, and σ is the spent charge in C. In (1) it is presumed that the applied battery current i_b is such that the battery voltage v_b reaches the cut-off value v_c at the total discharge time L, indicating a full discharge.

The consumed charge is represented in both (1) and (2) by the sum of two terms: the integral of the current signal, and a second term which gives the unavailable charge due to the formation of a charge gradient in the battery electrolyte as a result of the diffusion dynamics. This happens in the presence of a discharge current, and after it stops, the battery starts the recovery effect, where the gradient vanishes and the apparent charge of the battery increases. The diffusion model should be expected to accurately model this behavior.

$$\alpha = \int_0^L i_b(\tau)d\tau + 2\sum_{m=1}^{\infty}\int_0^L i_b(\tau)e^{-\beta^2 m^2 (L-\tau)}d\tau \quad (1)$$

$$\sigma(t) = \int_0^t i_b(\tau)d\tau + 2\sum_{m=1}^{\infty}\int_0^t i_b(\tau)e^{-\beta^2 m^2 (L-\tau)}d\tau \quad (2)$$

The battery state of charge A can then be defined as (3). Additionally, a steady-state solution for a constant current I can be obtained for(1)(Luiz et al. (2022)), resulting in (4). The diffusion model parameters α and β can be estimated using the steady-state solution by performing multiple constant current discharge experiments, a process which will be detailed in Section 4.

$$A(t) = 100\left(\frac{\alpha - \sigma(t)}{\alpha}\right)\% \quad (3)$$

$$\alpha = IL + \frac{\pi^2}{3\beta^2}I \quad (4)$$

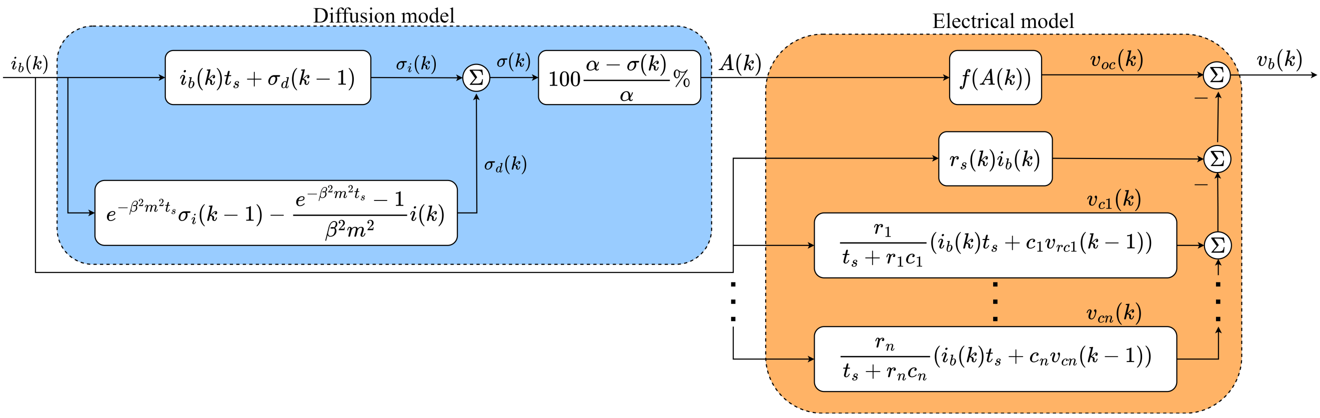

Fig. 1. Block diagram of the discrete battery model implementation.

3.2 Electrical model

The electrical model used is shown in Fig. 2. The battery voltage v_b is given by (5), where $v_{oc}(t)$ is the open-circuit voltage of the battery as a function of the state of charge $f(A(t))$, r_s is the series resistance. The voltage drop v_{rcj} for a given RC branch and is given by (6). These branches model the fast dynamics at the electrode of the battery, which aren't covered by the typically slower response of the diffusion model. This leads to the inclusion of these additional parameters in the model, as otherwise there would be non-modelled dynamics when comparing the experimental data with the model response for the battery voltage. The relationship between the open-circuit voltage v_{oc} and the state of charge A can be obtained through a low discharge rate experiment, for which (7) can be assumed as true.

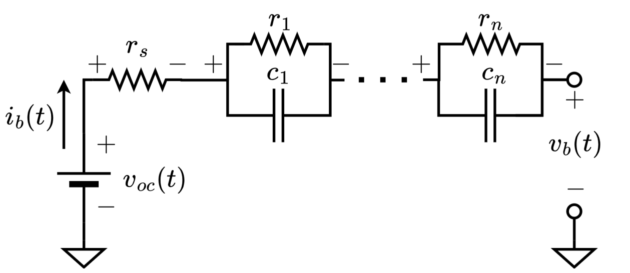

Fig. 2. Electrical model for a LiPo battery.

$$v_b(t) = v_{oc}(t) - r_s i_b(t) - \sum_{j=1}^{n} v_{cj}(t) \tag{5}$$

$$i_b(t) = \frac{v_{cj}(t)}{r_j} + c_j \dot{v}_{cj}(t) \tag{6}$$

$$v_b(t) \approx v_{oc}(t) \tag{7}$$

3.3 Discrete battery model

In order to apply an optimization algorithm to identify the model parameters, a discrete version of the complete battery model had to be implemented. The set of discrete equations for a given sampling time t_s using a trapezoidal approximation can be seen in (8), where σ_d is the delivered charge, σ_u is the unavailable charge and k is the discrete time. This model is derived from the equations for the diffusion and electrical models shown in Sections 3.1 and 3.2, respectively. A block diagram showing how the equations relate to one another is presented in Fig. 1 for added clarity.

$$\begin{aligned}
\sigma_d(k) =& i_b(k)t_s + \sigma_d(k-1)\\
\sigma_u(k) =& 2\sum_{m=1}^{M}\left(e^{-\beta^2 m^2 t_s}\sigma_u(k-1) - \frac{e^{-\beta^2 m^2 t_s} - 1}{\beta^2 m^2} i_b(k)\right)\\
\sigma(k) =& \sigma_d(k) + \sigma_u(k)\\
A(k) =& 100\frac{\alpha - \sigma(k)}{\alpha}\%\\
v_{oc}(k) =& f(A(k))\\
v_{cj}(k) =& \frac{r_j}{t_s + r_j c_j}\left(i_b(k)t_s + c_j v_{cj}(k-1)\right)\\
v_b(k) =& v_{oc}(k) - r_s(k)i_b(k) - \sum_{j=1}^{n} v_{cj}(k)
\end{aligned} \tag{8}$$

For the discrete model, the order M of the approximation of the infinite sum for the discrete diffusion model must be specified. In Neves et al. (2016) it was shown that for $M = 10$ is sufficiently precise while keeping the simulation cost as low as possible. In total, five constant parameters must be properly identified to model a given battery, two for the diffusion model and three for the electrical model, along with an expression for the open-circuit voltage as a function of the state of charge. As the involved dynamics are nonlinear and there are constraints on the parameter values, any optimization approach chosen for the identification process must be able to solve nonlinear constrained problems.

4. EXPERIMENTAL AND MODELLING RESULTS

This section describes the employed experimental setup and the performed tests, while also showing the performance of the identified models and of each of the optimization algorithms that were used. The estimation error,

ISSN: 2525-8311

DOI: 10.20906/CBA2022/3491

calculated as shown in (9), will be used as a metric to evaluate the results, in addition to its mean and the maximum values.

$$e = 100 \left| \frac{x_{data} - x_{estimated}}{x_{data}} \right| \% \tag{9}$$

4.1 Experimental setup

An EA-EL 9080-400 programmable DC load was used to set the discharge rate for each experiment, and an OWON XDM2041 digital multimeter was employed to measure the voltage at the cell terminals during the discharges. Both devices were connected to a computer through a serial connection, through which the collected data was transmitted. The resulting raw data files were exported to Matlab. A diagram of the setup can be seen in Fig. 3.

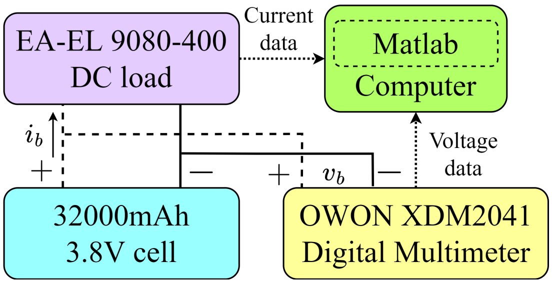

Fig. 3. Experimental setup used to collect battery discharge data.

The experimental data used for the model estimation was collected from three 3.8V 32000mAh cells. The use of multiple cells in the experimental stage helps to diminish any outlying characteristics that might be present in a single battery and also contributes to the generalization of the modelling results.

4.2 Experiment design

In Section 3, the model parameters were listed and the equations describing their behavior in the battery dynamics where shown. Analyzing these expressions, the following experiments were designed in order to estimate the corresponding parameters:

- Constant current discharges to identify the diffusion model constants α and β, starting at the nominal current value of the cells of $32A$, and then its multiples $64A$, $96A$, $128A$, $160A$ and $192A$, given that the maximum discharge current for these cells is $200A$.
- A constant current discharge at $3.2A$ in order to obtain a curve for the open circuit voltage v_{oc}.
- A pulsed current discharge, used at first to identify the electrical model parameters r_s, r_1 and c_1, and in a second moment to re-estimate the diffusion coefficient β. The pulses had an amplitude of $100A$, with a duration of $30s$ and a subsequent interval of 29 minutes and 30 seconds to allow for the regeneration of the battery voltage, for a total cycle duration of 30 minutes. Each cell was subjected to 34 cycles.

The voltage data for all experiments was sampled at $0.1s$, and the resulting raw data files were parsed and interpolated so as to obtain a time vector with equally spaced samples, since there are small variations in the sampling time of the measuring equipment.

4.3 Diffusion model estimation

The optimization problem for estimating α and β is described in (10), where L_{estim} is obtained from (4) and L_{data} is measured from constant current discharge experiments. The resulting pairs of current and discharge times from these experiments, along with the discharge time estimates obtained after estimating the values of α and β are shown in Fig. 4, with the corresponding estimation errors shown in Fig. 5.

$$\begin{aligned} & \min_{\alpha,\beta} \frac{1}{N} \sum_{k=1}^{N} (L_{data}(k) - L_{estim}(k))^2 \\ & \text{s.t.} \quad \alpha \geq 0 \\ & \qquad \beta \in [0, 1] \end{aligned} \tag{10}$$

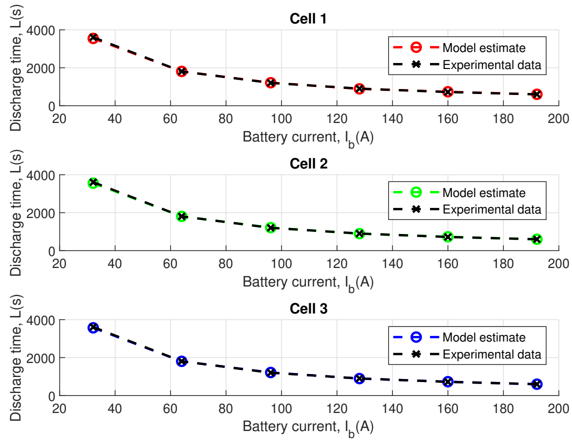

Fig. 4. Comparison between experimental data and model prediction for constant current discharge times.

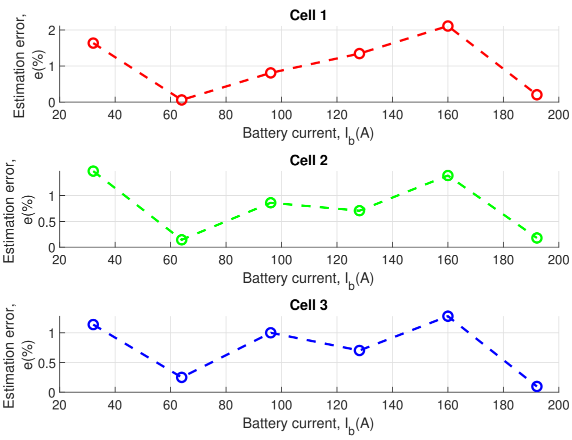

Fig. 5. Estimation error for constant current discharge times.

It's evident that the model is precise when it comes to predicting the discharge time for a given constant current, with the highest error among all cells being slightly over 2%. However, the prediction of the battery behavior must also be satisfied for the regeneration regime, which happens after the discharge ends and the charge gradient fades. When the modelling process came to the stage of verifying if this behavior was accurately represented, the results were not satisfactory, as can be seen in Fig. 6.

Further investigation revealed that since the diffusion coefficient had been estimated from a constant current response during a discharge, it didn't reflect the dynamics of the regeneration regime. This led to the proposal of estimating a new value for β from the pulsed current experiment data set, as the regeneration regime is well represented in that experiment.

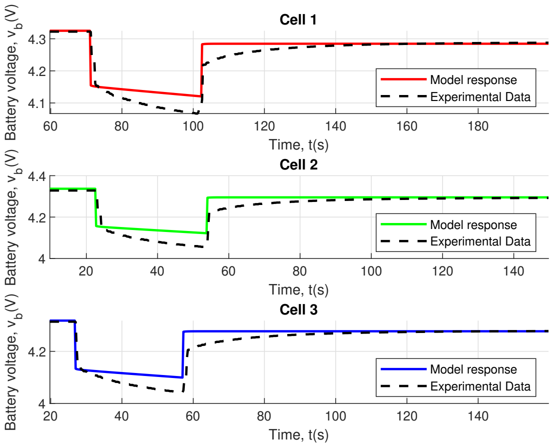

Fig. 6. Model response for the constant current estimated β.

4.4 Open circuit voltage estimation

When establishing the relationship between the open circuit voltage and the state of charge, a low current experiment may be performed. Since this current is constant, the steady state solution shown in (4) is valid, and, furthermore, the unavailable charge term can be considered negligible for small discharge rates. Therefore, the state of charge is approximately linear in this case. This is important because the state of charge for this modelling step can be obtained through the integration of the current signal alone, since it was already shown that the diffusion coefficient β obtained from the constant discharge experiments is not reliable, and therefore should not be used to estimate the state of charge for the open circuit voltage experiments.

This leads to an optimization problem between the voltage data measured during the experiment and the corresponding state of charge estimate, described in (11), where v_b^{data} is the voltage measured during the low current experiment, remembering that in this case (7) is a valid approximation. In this case, a choice must be made regarding the expression of the open-circuit voltage as a function of the state of charge $f(A(k))$. Three approaches were tested: a 9^{th} degree polynomial expression, a 7^{th} order Fourier series approximation and linear curve interpolation. The order of the mathematical expressions was chosen as the lowest order that gave a mean error under 1%, to avoid using high order expressions unnecessarily. Due to the long discharge times for a low current there are plenty of data points for the interpolation, meaning that linear interpolation can be chosen at no cost in modelling error instead of more complex interpolation algorithms.

The experimental data and the corresponding v_{oc} model curves for each cell can be seen in Figs. 7 to 9, as is their estimation error. The corresponding estimation error metrics for each cell are shown in Tables 1 to 3. It should be noted that this conclusion is a consequence of the long duration of this experiment, which generates an abundance of data points between which the interpolation can be calculated.

$$\min \frac{1}{N}\sum_{k=1}^{N}(v_b^{data}(k) - f(A(k)))^2 \tag{11}$$

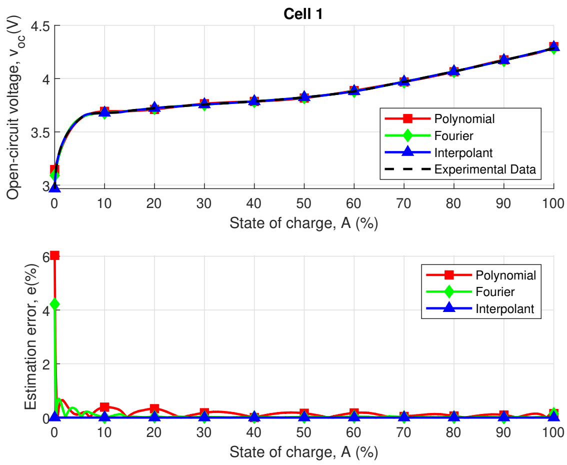

Fig. 7. Open circuit voltage estimation results for cell 1.

Table 1. Open circuit voltage estimation error metrics for cell 1.

	Mean error (%)	Maximum error (%)
Polynomial	0.149	6.031
Fourier	0.041	4.216
Interpolation	0.032	0.098

Table 2. Open circuit voltage estimation error metrics for cell 2.

	Mean error (%)	Maximum error (%)
Polynomial	0.165	6.066
Fourier	0.076	4.250
Interpolation	0.046	0.172

Table 3. Open circuit voltage estimation error metrics for cell 3.

	Mean error (%)	Maximum error (%)
Polynomial	0.173	5.845
Fourier	0.099	4.033
Interpolation	0.078	0.296

Analyzing the the error graphs in Fig. 7 to 9, it becomes clear that the curve interpolation approach is the best

ISSN: 2525-8311

DOI: 10.20906/CBA2022/3491

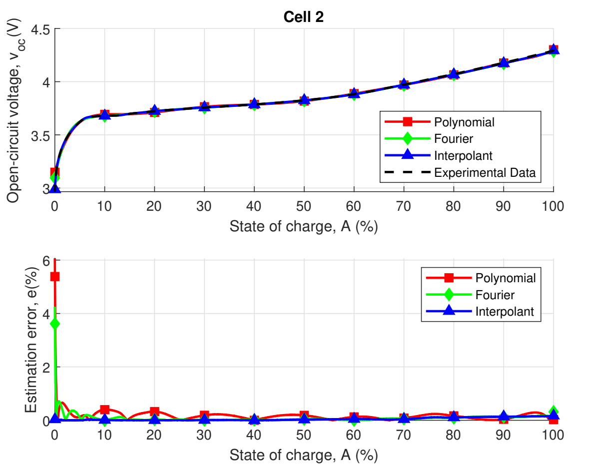

Fig. 8. Open circuit voltage estimation results for cell 2.

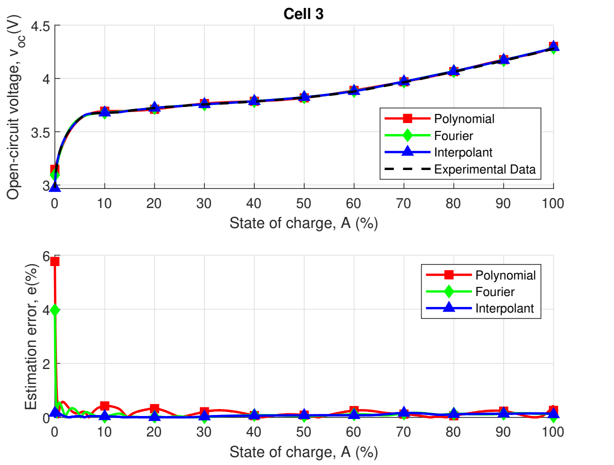

Fig. 9. Open circuit voltage estimation results for cell 3.

choice among the ones proposed, considering both the mean and maximum estimation error under 1% for all modelled cells. While all three approaches show a low estimation error for the mid to high values of state of charge, the polynomial and Fourier series expressions have a significantly worse performance for in the low state of charge band.

4.5 Electrical model and diffusion coefficient re-estimation

At this point, the pulsed current experiments are used to estimate the remaining model parameters: the electrical model constants and the diffusion coefficient β, which needs to be recalculated. This is the most computationally intensive step of the modelling process, due to the number of variables that need to be estimated, the size of the data set and the overall model complexity. The optimization problem to identify these parameters is stated in (12), with v_b^{data} being measured from the pulsed current experiments and v_b^{estim} being calculated from the discrete battery model from (8).

The number of RC branches used in the model is a subject of research unto itself (Ran et al. (2010)), but for our purposes a single branch was deemed enough to model the corresponding dynamics, as the addition of extra branches resulted in the increase of the parameter identification time at no significant increase in model precision. The inclusion of extra branches is particularly costly, as the related parameters do not have evident estimation bounds and providing initial values for the optimization algorithms demands previous system knowledge.

$$\begin{aligned} \min_{r_s, r_1, c_1, \beta} \; & \frac{1}{N}\sum_{k=1}^{N}(v_b^{data}(k) - v_b^{estim}(k))^2 \\ \text{s.t.} \; & r_s \geq 0 \\ & r_1 \geq 0 \\ & c_1 \geq 0 \\ & \beta \in [0, 1] \end{aligned} \tag{12}$$

Five numerical approaches have been chosen to be evaluated in this step, all of them widely employed in the scientific literature and capable of dealing with constrained nonlinear optimization: interior point method, sequential quadratic programming (SQP), active set, genetic algorithm with adaptive mutation and the Levenberg-Marquadt algorithm. All of the algorithms had a step tolerance of 10^{-6}, with the same initial values being used for the interior point, SQP, active set and Levenberg-Marquadt cases. The genetic algorithm had a population of 100 and a maximum number of generations of 1000 and the same error tolerance. These hyperparameters where chosen from a band between 20 and 200 for population and 500 to 2000 for number of generations, with the chosen values yielding a result under the error tolerance while being less time intensive than other higher values used.

The results for each of the three cells are presented in Figs. 10 to 12, with the estimation error mean and maximum values for each case shown in Tables 4 to 6. An observation must be made here, as the Levenberg-Marquadt results are not shown in the graphs. This happened because this algorithm had a very poor performance when compared to the other alternatives. Since its inclusion would just pollute the reading of the resulting graphs, a choice was made to omit them from these figures, presenting only the corresponding error metrics in the tables.

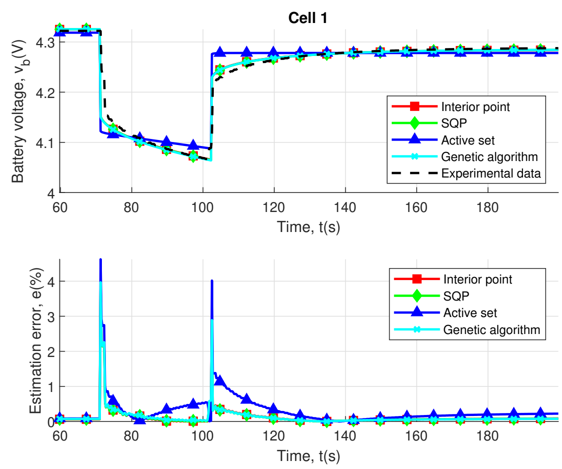

Fig. 10. Model responses for cell 1.

When evaluating the performance of the obtained models and the corresponding optimization algorithms, the most

Table 4. Battery voltage estimation error metrics for cell 1.

	Mean error (%)	Maximum error (%)
Interior point	0.120	3.962
SQP	0.119	3.954
Active set	0.290	4.624
Genetic algorithm	0.122	3.968
Levenberg-Marquadt	14.918	19.710

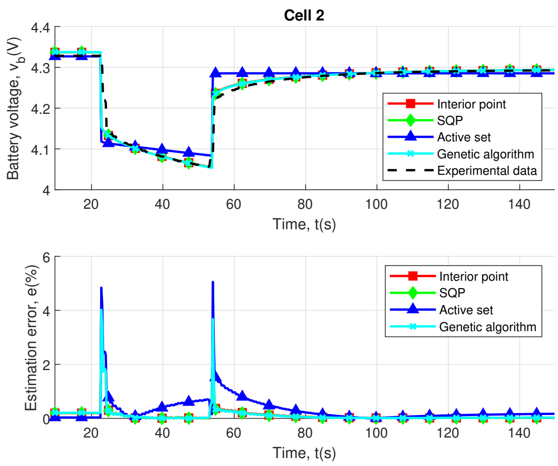

Fig. 11. Model responses for cell 2.

Table 5. Battery voltage estimation error metrics for cell 2.

	Mean error (%)	Maximum error (%)
Interior point	0.111	4.050
SQP	0.108	4.033
Active set	0.310	5.051
Genetic algorithm	0.107	4.027
Levenberg-Marquadt	16.257	21.967

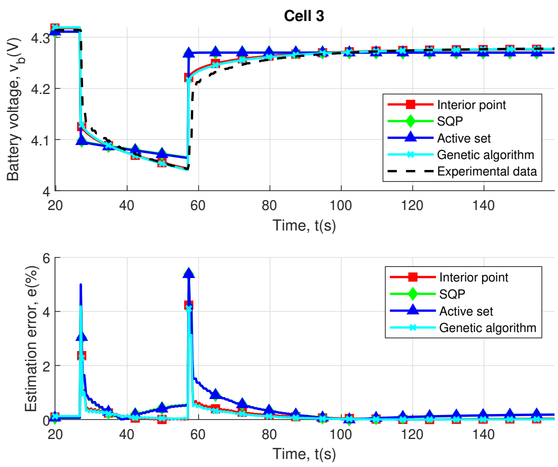

Fig. 12. Model responses for cell 3.

important factor is how well the physical dynamics of the battery were represented. Additionally, it's desirable for the modelling approach to be applicable to any LiPo battery, provided that the necessary experimental data is available. Keeping these factors in mind, it's visible that the active set approach was fair, but had the worst performance among the other approaches.

Table 6. Battery voltage estimation error metrics for cell 3.

	Mean error (%)	Maximum error (%)
Interior point	0.150	4.277
SQP	0.325	5.380
Active set	0.324	5.375
Genetic algorithm	0.130	4.188
Levenberg-Marquadt	17.149	24.082

The interior point, SQP and genetic algorithm identified models had a mostly similar behavior across all three cells, presenting a mean estimation error under 1% and a maximum estimation error of around 5% in the transient response. This shows that the combination of the Rakhmatov-Vrudhula diffusion model and the electrical model can accurately represent the behavior for these cells.

At a closer inspection, it can be seen that the SQP model for Cell 3 had metrics similar to that of the active set alternative. This can be either due to a specific characteristic of this cell manufacturing or to a particularity of the data set which made the algorithm settle for a local minimum, but since the interior point and genetic algorithm didn't suffer the same problem, they should be considered over the SQP approach, so that the resulting model is less prone to error due to such factors.

The choice between the interior point and genetic algorithm can be guided by their metrics during the optimization process, which can be seen in Table 7, which show the time it took each algorithm the estimate the model parameters. The genetic algorithm was by far the slowest, taking more than 2 hours to run in some cases, while the interior point approach ran under a minute with no significant loss in model accuracy. However, the genetic algorithm has the advantage of not needing an initial point to be set. This is important because the choice of an initial guess is critical for the interior point algorithm, and the knowledge of what constitutes a good starting point for the optimization demands either an iterative process or previous knowledge of the system parameters. Therefore, if during the modelling process a reasonable guess can be made regarding the values of the parameters, the active set algorithm should be used, with the genetic algorithm being the choice otherwise, unless the long optimization time is prohibitive for the intended application.

Table 7. Execution time for the optimization algorithms.

	Cell 1	Cell 2	Cell 3
Interior point	36.392s	44.559s	31.272s
SQP	16.486s	14.931s	6.832s
Active set	6.103s	6.042s	5.916s
Genetic algorithm	6882.383s	1468.587s	2332.450s
Levenberg-Marquadt	57.732s	59.074s	58.795s

5. CONCLUSION

A model for a LiPo battery was proposed and implemented, modelling both the lithium diffusion and electrode dynamics. The model was shown to be capable of modelling these behaviors. Several modelling strategies regarding the optimization process for the model parameters identification were explored and the use of either an active set or a genetic algorithm coupled with a curve interpolation for the open circuit voltage had the best performance.

Future research avenues are possible by aiming to improve model performance, particularly for the transient response, and exploring the inclusion of effects such as temperature and aging. As the developed model is not computationally intensive, it's also possible to study its inclusion to model-in-the-loop approaches for embedded system designs, such as applications in unmanned aerial vehicles and other systems that typically use LiPo batteries as their power source. Finally, there are models which use electrochemical approaches in place of the electrical circuit used in this paper, and a comparison between the behavior of these alternatives might be of interest.

REFERENCES

Afshari, H.H., Attari, M., Ahmed, R., Delbari, A., Habibi, S., and Shoa, T. (2018). Reliable state of charge and state of health estimation using the smooth variable structure filter. *Control Engineering Practice*, 77, 1–14. doi:10.1016/j.conengprac.2018.04.015. 2

Barcellona, S. and Piegari, L. (2021). Integrated electro-thermal model for pouch lithium ion batteries. *Mathematics and Computers in Simulation*, 183, 5–19. doi:10.1016/j.matcom.2020.03.010. 2

Chen, M., Zhang, L., Yu, F., and Zhou, L. (2019). An aging experimental study of li-ion batteries for marine energy power station application. In *Conf. Rec. IEEE/PHM-Qingdao*, 1–6. doi:10.1109/PHM-Qingdao46334.2019.8942865. 2

Cipin, R., Toman, M., Prochazka, P., and Pazdera, I. (2019). Identification of li-ion battery model parameters. In *International Conference on Electrical Drives Power Electronics (EDPE)*, 225–229. doi:10.1109/EDPE.2019.8883926. 1

Daigle, M. and Kulkarni, C.S. (2013). Eletrochemistry-based batery modeling for prognostics. In *Conf. Rec. PHM*. doi:10.36001/phmconf.2013.v5i1.2252. 1, 2

Doyle, M., Fuller, T.F., and Newman, J. (1993). Modeling of galvanostatic charge and discharge of the lithium/polymer/insertion cell. *Journal of The Electrochemical Society*, 140(6), 1526–1533. doi:10.1149/1.2221597. 1, 2

Guo, Z.M., Huang, S.M., and Tsai, T.H. (2019). A current-mode control li-ion battery charger with trickle-current mode and built-in aging detection. In *Conf. Rec. IEEE/ISCAS*, 1–4. doi:10.1109/ISCAS.2019.8702384. 2

Junhuathon, N., Sakunphaisal, G., and Chayakulkheeree, K. (2020). Li-ion battery aging estimation using particle swarm optimization based feedforward neural network. In *Conf. Rec. IEEE/ICPEI*, 73–76. doi:10.1109/ICPEI49860.2020.9431432. 2

Lee, K.T., Dai, M.J., and Chuang, C.C. (2018). Temperature-compensated model for lithium-ion polymer batteries with extended kalman filter state-of-charge estimation for an implantable charger. *IEEE Trans. Ind. Electron.*, 65(1), 589–596. doi:10.1109/TIE.2017.2721880. 2

Luiz, S.O.D., Lima, E.G., and Lima, A.M.N. (2022). Representing the accumulator ageing in an automotive lead-acid battery model. *J Control Autom Electr Syst*, 33, 204–218. doi:10.1007/s40313-021-00803-z. 2

Mazumder, S. and Zhang, S.S. (2013). Faster-than-real-time simulation of lithium ion batteries with full spatial and temporal resolution. *International Journal of Electrochemistry*, 2013. doi:10.1155/2013/268747. 2

Muratori, M., Canova, M., Guezennec, Y., and Rizzoni, G. (2010). A reduced-order model for the thermal dynamics of li-ion battery cells. *IFAC Proceedings Volumes*, 43(7), 192–197. doi:10.3182/20100712-3-DE-2013.00190. Conf. Rec. IFAC/AAC. 2

Neves, B.H., Vilar, B.M., Silva, F.d.M., Luiz, S.O., Silva, J.J., and Perkusich, A. (2016). Battery lifetime estimation by means of an analytical continuous-time model. In *Conf. Rec. IEEE/INDUSCON*, 1–5. doi:10.1109/INDUSCON.2016.7874498. 1, 2, 3

Peng, W., Yang, Z., Liu, C., Xiu, J., and Zhang, Z. (2018). An improved pso algorithm for battery parameters identification optimization based on thevenin battery model. In *2018 5th IEEE International Conference on Cloud Computing and Intelligence Systems (CCIS)*, 295–298. doi:10.1109/CCIS.2018.8691341. 1

Rakhmatov, D. and Vrudhula, S. (2001). An analytical high-level battery model for use in energy management of portable electronic systems. In *Conf. Rec. IEEE/ACM/ICCAD*, 488–493. doi:10.1109/ICCAD.2001.968687. 1, 2

Ran, L., Junfeng, W., Haiying, W., and Gechen, L. (2010). Prediction of state of charge of lithium-ion rechargeable battery with electrochemical impedance spectroscopy theory. In *Conf. Rec. IEEE/ICIEA*, 684–688. doi:10.1109/ICIEA.2010.5516984. 6

Schmidt, A.P., Bitzer, M., Árpád W. Imre, and Guzzella, L. (2010). Lumped parameter modeling of electrochemical and thermal dynamics in lithium-ion batteries. *IFAC Proceedings Volumes*, 43(7), 198–203. doi:10.3182/20100712-3-DE-2013.00010. 6th IFAC Symposium on Advances in Automotive Control. 1, 2

Spohn, M.A., Sausen, P.S., Salvadori, F., and Campos, M. (2008). Simulation of blind flooding over wireless sensor networks based on a realistic battery model. In *Conf. Rec. IARIA/ICN)*, 545–550. doi:10.1109/ICN.2008.100. 2

Valladolid, J.D., Patiño, D., Ortiz, J.P., Minchala, I., and Gruosso, G. (2019). Proposal for modeling electric vehicle battery using experimental data and considering temperature effects. In *Conf. Rec. IEEE/PowerTech*, 1–6. doi:10.1109/PTC.2019.8810611. 1, 2

Wang, C., Xu, M., Zhang, Q., Jiang, R., Feng, J., Wei, Y., and Liu, Y. (2022). Cooperative co-evolutionary differential evolution algorithm applied for parameters identification of lithium-ion batteries. *Expert Systems with Applications*, 200, 117192. doi:10.1016/j.eswa.2022.117192. 2

Wang, Y., Li, M., and Chen, Z. (2020). Experimental study of fractional-order models for lithium-ion battery and ultra-capacitor: Modeling, system identification, and validation. *Applied Energy*, 278, 115736. doi:10.1016/j.apenergy.2020.115736. 2